Dalton Transactions

Accepted Manuscript

ROYAL SOCIETY OF CHEMISTRY

www.rsc.org/dalton

Journal Name

ARTICLE

Photo-activated CO-Releasing Molecules (PhotoCORMs) of Robust Sawhorse Scaffolds [μ^2-OOCR^1, η^1-$NH_2CHR^2(C=O)OCH_3$, $Ru(I)_2CO_4$]

Received 00th January 20xx,

Accepted 00th January 20xx

DOI: 10.1039/x0xx00000x

www.rsc.org/

Shuhong Yang, Mengjiao Chen, Lingling Zhou, Guofang Zhang, Ziwei Gao and Weiqiang Zhang*

A class of sawhorse-type ruthenium (I) featuring a stable CORM sphere with diverse carboxylic and amino acid derivatives were synthesized and validated as lead structures for photo-activated CO-releasing molecules (PhotoCORMs). The CO release of these CORMs were triggered by 365nm UV irradiation. The cell viability studies indicated that **3a** and **3f** were non-toxic both in dark and UV light, making them excellent lead structures for the therapeutic CORMs.

Introduction

The photolysis of metal carbonyls complexes has been developed as an efficient way to delivery carbon monoxide (CO) for therapeutic application including anti-inflammation, vasodilatation, anti-apoptosis, anti-proliferation and anti-Hypoxia.[1] To achieve precise temporal and spatial control on CO liberation under physiological condition, both CORM and drug spheres of photo-activated CO releasing molecules (PhotoCORMs) have been devised to satisfy the critical ADMET (Absorption, Distribution, Metabolism, Excretion and Toxicity) requirements of CO pro-drugs.[2] In CORM sphere, various multi-dentated ligands[3,4] were introduced to finely tune the dissociation of carbonyl ligands; In drug sphere, the hydrophilic small and macro molecules[5,6] were tethered to enhance their water-solubility and potentially achieve targeted CO release.[7] Despite a large collection of transition metal carbonyls with different ligands had their ADMET properties extensively examined, most of CO therapeutic experiments relied on the simple ruthenium(II) carbonyl, $[RuCl(\mu^2\text{-}Cl)(CO)_3]_2$ (CORM-2), as solid form of CO resource.[8] In fact, few biological active CORMs with ML_6 octahedral scaffolds, such as $[RuCl(glycinato)(CO)_3]$ (CORM-3),[9] $[Mo(glycinato)(CO)_5]$,[10] and $[Mo(isocyaonacetate)(CO)_3]$ (AFL794)[11] were studied in the animal tests of pre-clinic CO therapy. To explore new scaffolds of low toxic metals and hydrophilic coordination sphere is highly desirable for developing therapeutic CORMs.[12,13]

Water-soluble CORM-3 is the cornerstone in the therapeutic application of CORM. In the CORM sphere of CORM-3, the chelated glycinate ligand successfully regulates the degrade of $[Ru(CO)_3Cl]$ fragment, but also increases the water-solubility of hydrophobic metal carbonyl moiety.[13] In spite of a recent contradictory report on its sophisticated CO release pathway,[14] the low toxicity and a variety of beneficial therapeutic effects of CORM-3 inspired the extensive research on lead structures based on $[Ru^{II}(CO)_xL_y]$.[10] A recent study found that in aqueous medium, the chemistry of $Ru^{II}(CO)_3Cl_2L$ complexes were governed by the reactivity of the metallacarboxylate species which firstly release CO_2 instead of CO. We hypothesized that Ru^{I} as central metal might form more robust Ru-CO bonds and therefore, circumvent the water-gas shift conversion of Ru^{II} carbonyl complexes. Herein, we reported Ru^{I} sawhorse complexes $[Ru(\mu^2\text{-carboxylato})(L)_2(CO)_2]_2$ as new scaffold for CO delivery *in vitro.* The sawhorse ruthenium complexes were of great interest as metallo therapeutic agent due to low toxicity of ruthenium and therapeutic effect of CO. Accordingly, their potentials as CORM were proposed by B. Therrien[15] and G. Süss-Fink[16] recently. Until now, PhotoCORMs relied on N, S chelating ligands to modulate their CO release under physiological condition (Scheme 1). For instance, cysteamine (N,S) of CORM-S1 stabilized $[Fe(II)CO_2]$ unite, which is suitable for selective CO release and possesses a high potential for therapeutic application.[3] Tris(pyrazolyl)methane (N,N,N) were employed to prepare light-activatable cytotoxic agent of $[Mn(CO)_3]$ unit with photolabile CO ligands.[12] The hard donor O ligands like acetic acid, amino acids and their derivatives were rarely employed for PhotoCORMs design although these hydrophilic molecules were natural abundant, nontoxic and beneficial to

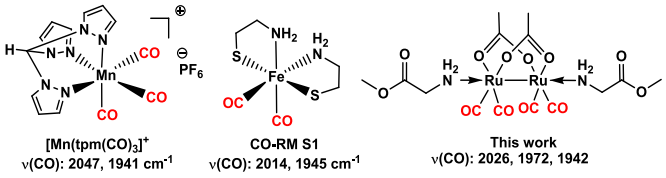

Scheme 1. Lead structures for PhotoCORMs.

[a] S. H. Yang, M. J. Chen, L. L. Zhou and Prof. W. Zhang, Key Laboratory of Applied Surface and Colloid Chemistry, MOE, School of Chemistry and Chemical Engineering Shaanxi Normal University, Xi'an 710062 (China) Fax: +86-29-81530727(+)E-mail: zwq@snnu.edu.cn

† Electronic Supplementary Information (ESI) available: Sample preparation and spectroscopic (UV absorption, TG-DSC, FT-IR, NMR and HR ESI-MS). See DOI: 10.1039/x0xx00000x

enhance the water-solubility of CORM. Another advantageous of the sawhorse scaffold is that a large variety of carboxylic acids and their derivatives diversify the ligand choice at both equatorial and axial position, which is essential for the optimization of the molecular structures of CO pro-drugs.

Results and discussion

Synthesis and characterization of 3a-3g

We firstly screened the CO releasing profile of well-known acetate bridged sawhorse-type complex with phosphine at axial positions. Preliminary experiments found that sawhorse diruthenium(I) tetracarbonyl bearing PPh_3 was too stable to be photo-activated and release CO in standard horse heart myoglobin (Mb) assay. To our surprise, by simply replacing the phosphine ligand by more hydrophilic glycinate esters, the new simple ruthenium carbonyls **3a** released CO in well-controlled manner.

Since their discovery in 1969, a considerable number of sawhorse structures of $Ru_2(CO)_4(O(C=O)R)_2L_2$ have been synthesized and used for catalysis and therapeutic application.[16] According to literature method,[17] we adopted a facile one-pot method to construct the sawhorse scaffold (Scheme 2.). The thermolysis of $Ru_3(CO)_{12}$ **1** with carboxylic acids at 110~130 °C for 8 hours afforded polymeric intermediate 2. At 50 °C, amino acid esters were added to occupy the axial position of **2**, which flourished the sawhorse scafforlds of **3**. Ruthenium complexes **3a-g** were synthesized and isolated in 74~87% yields as light yellow solids, which were stable and easily manipulated without any proof from moisture, oxygen or light. IR spectrum of Ru(I) complexes exhibited three terminal Ru-CO stretchings at 2027-1941 cm^{-1} and the carbonyl stretching of bridged-carboxylato ligand at 1590 cm^{-1}. The absorption of Ru-CO bonds (**3a-g**) are lower than the corresponding values of CORM-3,[15] indicating that more d electron back-donating from Ru(I) strengthen Ru-CO bonds. The NMR analysis revealed the structures of these ruthenium complexes in details. In ^{1}H-NMR spectrum of **3a**, for instance, the bridged-acetate was observed as a singlet at δ 1.96ppm. CH_2 and OCH_3 of axial glycine ester appeared as a triplet and singlet at δ 3.72 and 3.80 ppm, respectively. The $^{13}C\{^1H\}$ NMR spectra of **3a** showed the signals for the terminal carbonyl groups (Ru-CO) at δ 204 ppm and the carbonyl of μ^2-η^2-$OC(=O)CH_3$ at δ 172 ppm, respectively. Arylcarboxylato-bridged ruthenium complexes **3b-3g** showed the similar resonances of both bridged and axial ligands. Notably, the chemical shifts of NH_2 groups at the axial positions varied significantly, which might probe the coordination of η^1-glycinate ester ligands. The amino protons of μ^2-acetato complexes **3a** appeared at δ 2.87 ppm, and lower than of the corresponding chemical shift of μ^2-arylcarboxylato complexes **3b-3g**. The shielded amino proton of **3a** reflects less electron donating to sawhorse unit, indicating the corresponding axial ligand is more labile.

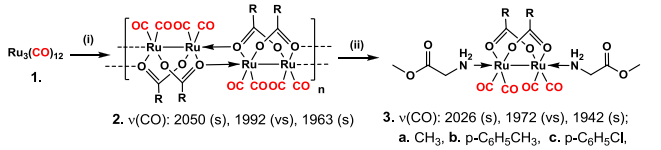

Scheme 2. Synthesis of carboxylato-bridged $Ru_2(CO)_4$ complexes of 3a-3g; (i) RCO_2H (3 equiv.), toluene, reflux; (ii) Glycine methyl ester (3 equiv.), CH_2Cl_2, 0 °C.

Crystallography

Yellow crystals of four diruthenium (I) complexes **3a**, **3d**, **3e** and **3f** grew from the diffusion of hexane to CH_2Cl_2 solution of complexes at 0 °C. The molecular structures of these complexes were investigated by single crystal X-ray diffraction. Complexes **3a** and **3e** were selected to demonstrate the molecular feature of sawhorse skeletons bearing unique amino acid ester at axial position (Fig. 1). The Ru-CO bond length of each terminal carbonyl is slightly different. For instance, the average Ru-CO bond length of these complexes is about 1.83 Å, much shorter than Ru-CO (1.943(3) Å and 1.903(3) Å) of CORM-3,[15] but longer than Ru-CO (1.76 Å) bonds of triphenylphosphine analogues.[16] These crystallography observations rationalize the well-controlled CO releasing of **3a** in Mb assay. As for bridged ligands, the distances between Ru and O of μ^2-acetato ligand is 2.12 Å, while μ^2-bezonato ligand coordinates tighter (average Ru-O 2.10 Å). The benzene rings of bridged aromatic carboxylic acids might delocalize more d electron density from sawhorse $Ru_2(CO)_4$ unite. At same time, the electron delocalization can also reduce the back-donation from $Ru_2(CO)_4$ to π* orbital of carbonyl ligand. As a consequence, the weaker Ru-CO bonds might exist in μ^2-arylcarboxylato bridged complexes **3d**, **3e** and **3f**. Finally, two axial N donor ligands coordinate to sawhorse unite $Ru_2(CO)_4$ unequally in solid state. In complex **3a**, Ru(1)-N(1) 2.248(3) Å is shorter than Ru(2)-N(2) 2.263(2) Å.

Interestingly, the packing structures of these sawhorse ruthenium complexes were strongly influenced by extensive H-bondings. In all cases (ESI, Table S3), both intermolecular and intramolecular H-bondings were observed between the axial

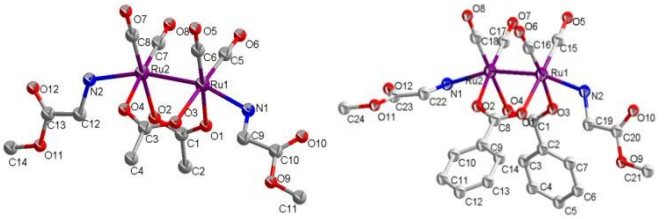

Fig. 1 Molecular structures of diruthenium complexes, 3a (left) and 3e (right); H-atoms and solvent omitted for clarity.

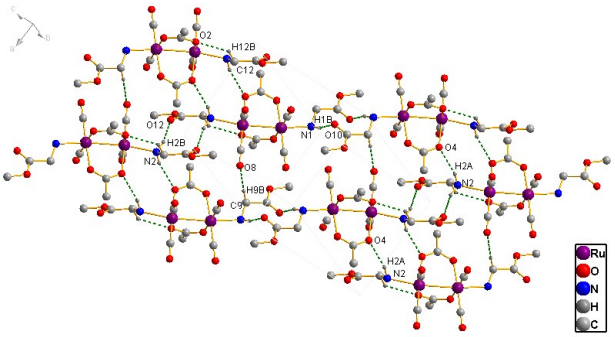

Fig. 2 Ball-and-stick diagram of the extended structure of 3a viewed down the a axis. Dashed lines indicate hydrogen bonding.

amino groups, the oxygen atoms of ester group and μ^2-acetato group in a neighboring molecule, respectively. As shown by μ^2-acetato bridged complexes **3a** (Fig. 2), the hydrogen bonds of axial amino group and ester group (N1-H···O10 2.23(4) Å) formed a one-dimensional chain network along the c axis. The hydrogen bonds between another amino group with oxygens of μ^2-acetato (N(2)-H(2A)···O(4) 2.32(Å) and N(2)-H(2A)···O(12) 2.30 (Å) were shorter. The complex 2D network was built up from these hydrogen-bonded sheets. Although this is a common feature to all the solid state structures in this series compounds, the hydrogen bonds are unlikely to persist in the aqueous medium employed for the CO-release measurement.

CO release measurement via myoglobin assay

All ruthenium (I) complexes were extremely stable toward physiological releasing triggers, hydrolysis, thermolysis (37.8 ^{o}C) and thiol donors (sodium dithionite). In aerated solutions, such as DMSO, H_2O and ethanol, the characteristic IR absorption of these CORMs unchanged after at least 24 hours storage at 25 ^{o}C without any lightproof. The standard myoglobin assay tests confirmed that these ruthenium complexes did not release CO. The deoxy-Mb → Mb-CO conversion cleanly occurred on UV irradiation of **3a** with four isosbestic points (Fig. 3). 60 μM of **3a** saturated deoxyMb solution after 1600 s, and 40 μM of **3a** delivered at least 50 μM of carbon monoxide after 2400 s. The CO-releasing kinetics of these CORMs with $t_{1/2}$ and $t_{1/4}$ values were measured and listed in Table 1. A wild range of CO-releasing rates were observed when the bridged ligands of **3a-3g** vary from acetato- to arylcarboxylato-, demonstrating the tunable CO releasing of these simple ruthenium complexes for therapeutic application.

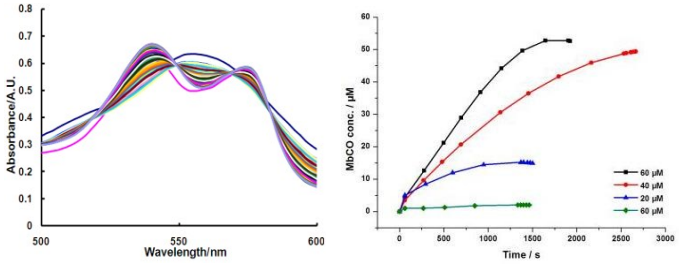

Fig. 3 UV-vis spectrum showing the Q-bands during the conversion of deoxy-Mb to MbCO with time for a 60 μM solution [PBS pH= 7.4, 37.8 ^{o}C] (**Left**); Deoxy-Mb → Mb-CO conversion time – photochemical induced release of CO using an LED (at 360 nm, 5 W) from **3a** [c = 20 μM (blue), 40 μM (red), 60 μM (black) and 60 μM (green, control experiment without UV irradiation)] (**Right**).

Table 1. IR, NMR and CO releasing kinetics of Complexes 3a-3f

Entry	V(CO) [a]	δ(NH$_2$) [b]	*t*		
			60 μM	40 μM	20 μM
3a	2026,1972,1941	2.87	724[c]	665[c]	414[c]
3b	2025,1972,1941	3.14	1682[d]	2207[c]	1250[c]
3c	2027,1974,1944	3.14	2007[d]	2318[c]	1733[d]
3d	2024,1971,1941	3.13	1852[c]	1373[c]	1766[c]
3e	2026,1973,1943	3.16	2220[c]	1291[c]	1239[c]
3f	2027,1972,1943	3.04	1951[d]	921[d]	1723[d]
3g	2026,1972,1942	3.08	2042[d]	1493[d]	1640[c]

[a] IR spectra were record in DCM, cm^{-1}; [b] ^{1}H-NMR were record in $CDCl_3$, ppm; Kinetics measured with standard myoglobin assay as [c] $t_{1/2}$ and [d] $t_{1/4}$, s.

The spectroscopic data of ruthenium (I) complexes **3a-3f** were correlated to their CO releasing kinetics in Table 1. The Ru-CO stretchings of **3a-3f** were basically identical, ruling out the dissociation of CO as the rate-determined step. **3a** released CO far more rapidly than their aromatic analogues **3b-3f**, whilst the amino protons of **3a** were observed at δ 2.87 ppm, lower than others. Since the chemical shifts of amino protons can probe the coordination of axial ligand, the lability of the axial ligands, rather than carbonyl ligand, might be responsible for the whole releasing process. The further comparison of releasing kinetics of **3b-3f** revealed that the hydrophilicity was another factor controlling CO release in aqueous system. Ortho-methoxy on bridged ligand (**3d**) significantly promoted CO releasing with $t_{1/2}$, 40 μM of 1373 s. In contrast, none of methyl at ortho- (**3b**), para- (**3f**) and meta- (**3g**) position accelerated CO release faster than μ^2-benzato bridged **3e** with $t_{1/2}$, 40 μM of 1291 s. The correlation indicated that the CO releasing of sawhorse CORMs could be tuned by varying the bridged carboxylate ligands.

CO Release pathway

To get insights into the reactivity of these CORMs, the degradation of **3a** in both solid state and in solution were investigated by TG-DSC, FT-IR, ^{1}H-NMR and HR ESI-MS. TGA-DSC experiments proofed a remarkable thermal stability of **3a** (ESI, Fig. S4). Heating below 100 ^{o}C under N_2 flow, **3a** was stable without any mass losing. The first two mass lost of 13.58 % and 14.59 % were observed at 117.68 ^{o}C and 168.21 ^{o}C, respectively. These can be accounted for the dissociation of each axial ligand (14.59 % cal.). To our surprise, CO liberation process did not happen until polymeric sawhorse $Ru_2(CO)_4$ skeleton collapsed over 250 ^{o}C, along with losing a acetic anhydride and four molecules of CO. The corresponding mass lost was observed as 35.74 %, consistent with the experimental value of 35.05 %. The inorganic residue was collected and subjected to XPS analysis, revealing RuO_2 as inorganic degradation product (ESI，Fig S5).

The photolysis of **3a** in solution states were followed by FT-IR and ^{1}H-NMR. The characteristic M-CO absorption of **3a**

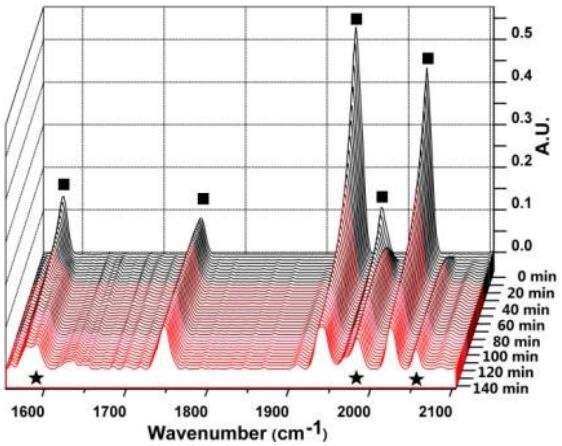

Fig. 4. FT-IR (ν(CO) region) of complex **3a** in acetonitrile solution and the changes that occur during 365 nm photolysis. **3a** (■), ν(CO): 2023, 1968 and 1936 cm^{-1}; photo product II (★) ν(CO):2055, 1984 and 1590 cm^{-1}.

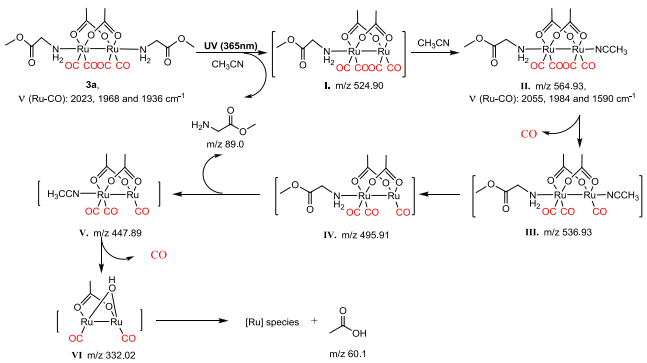

Scheme 3. A possible mechanism underlying the CO-releasing from **3a** and the fate of its non-carbonyl ligands after photolysis.

gradually decreased during UV irradiation (ESI, Fig. S6 and S7).

Interestingly, in acetonitrile, the photolysis of **3a** generated a new ruthenium carbonyl species. Difference spectrum between **3a** and the photo product **II** was shown in Fig. 4. The disappearance of the bands at 2023, 1968 and 1936 cm^{-1} and the growth of three new bands at 2055, 1984 and 1590 cm^{-1} suggested a dramatic change of the coordination sphere of **3a**. The shifts of the ν(CO) bands to higher frequency were consistent with the replacement of one labile axial ligand with more electron-withdrawing solvent ligand. No changes at 1749 cm^{-1} might result from the fast ligand exchange of dissociated and coordinated glycine methyl ester. To characterize photoproduct, the photolysis of **3a** in CD_3CN was followed by ^{1}H-NMR (ESI, Fig. S8). Upon UV irradiation, the singlet (δ 1.92 ppm) of acetato group in **3a** shifted downfield to δ 2.16 ppm which might be assigned as the protons of bridged ligand in photo product **II**. This NMR results were consisted with IR change at the range from 1600-1650 cm^{-1}.

To further identify these intermediates, the photolysis of **3a** in CH_3CN was monitored by ESI-MS. Under mass condition, **3a** formed an adduct with solvent molecules as the fragment peak at m/z 691.01(**3a·2CH$_3$CN**). The photolysis for 10 minutes consumed the adduct gradually. The further UV for 35 minutes generated several degraded ruthenium carbonyl fragments (**I.-VI.**) via photo-activated ligand dissociation of **3a**. (ESI, Fig. S10).

Taken together, these mechanistic experimentation shed light on the CO releasing pathway (Scheme 3.). The photolysis of complex **3a** initiated a rapid dissociation of axial ligand, confirmed by the fragment peak **I** at m/z 524.90. In acetonitrile, intermediate **II** (m/z 564.93) formed instantaneously and was also observed in both FT-IR and ^{1}H-NMR experiments. After that, the first CO released from the sawhorse scaffold $Ru_2(CO)_4$. Intermediate **III** formed, which can be assigned as fragment peak at m/z 536.93. The sequential dissociation of solvent and another axial ligand led to tricarbonyl sawhorse fragment **V** (m/z 447.89). The decarbonylation and hydrolysis of **V** released another CO and free acetic acid. The sawhorse unite converted to a bridged hydroxy intermediated **VI** (m/z 332.02). GC-MS analysis unveiled the fate of noncarbonyl ligands as free acetic acid and glycine methyl ester in the photolysis experiment. In contrast, no any other organic molecule was detected in control experiments without photolysis (ESI, Fig. S9).

Cytotoxicity studies

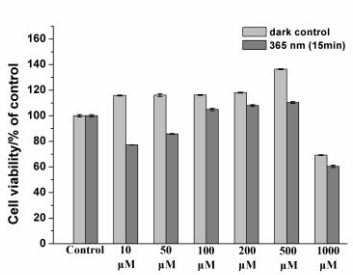

Fig. 5. Cell viability of RAW264.7 cell in presence of **3a**. Cells were grown in the presence of **3a** (10-1000 μM) and left in the dark (left) or Irradiated at 365 nm for 15 min (right).

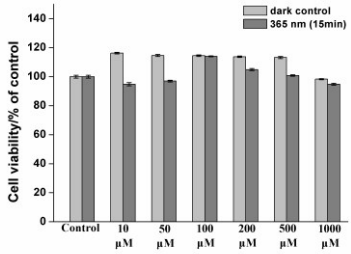

Fig. 6. Cell viability of RAW264.7 cell in presence of **3f**. Cells were grown in the presence of **3a** (10-1000 μM) and left in the dark (left) or Irradiated at 365 nm for 15 min (right).

To evaluate the cytotoxicity of sawhorse-type CORMs, the effect of **3a** and **3f** on the murine macrophages as were studied by MTT assay.[18] The cell culture of RAW264.7 was incubated with two CORMs, respectively for 24h in the presence of CO_2 and with water as control. Afterward, cells were irradiated for 15min with 365 nm light or left in the dark. After an additional 8h of growing all cells in the dark, the cell viability was determined using the MTT assay (Fig. 5 and 6). Control experiments with a water as blank confirmed that irradiation alone has no effect on the cell viability. Cells treated with **3a** and **3f** in the dark did not show a concentration-dependent loss of viability within the range of 10-500 μM. As high as 1000 μM of **3a** reduced the amount of cell biomass to about 69%. Upon irradiation, 10 μM **3a** inhibited the cell viability sightly. As the concentration of **3a** increased, the cell growth increased. The irradiation of **3a** surveyed 100-500 μM had no inhibition effect on the cell growth (Fig. 5). The bioactivity of **3f** is not photo-inducible. In presence of 10 μM to 1000 μM of **3f**, the viability of cell did not lose significantly (Fig. 6).

Conclusions

In conclusion, a new lead structure of PhotoCORM with simple ligand system was established by natural abundant carboxylic acids and its derivatives. To satisfy the pharmaceutical requirements, the clinic pro-drug of PhotoCORMs can be derived by varying both bridged and axial ligands. These sawhorse complexes are robust in both solid and solution states. Under the physiological condition, these CORMs do not reacted with oxygen, water, sodium dithionite.

Their CO liberation was only triggered by LED UV radiation. Notably, nontoxic acetic acid and glycine methyl ester were the photo products of **3a**. The mechanistic experimentation clearly demonstrated a well-defined degradation pathway, in which the dissociation axial ligand is the rate-determining step of the photoactiviated CO releasing. In cell viability experiment of murine macrophages as, these CORMs showed no cytoxicity. The toxicological and pharmacokinetic studies are under way to fully assess the toxicity and bio-distribution of these CORMs in animal models.

Experimental section

General

All manipulations were accomplished with standard Schlenk techniques. Decacarbonyl triruthenium ($Ru_3(CO)_{12}$) and glycine methyl ester ($GlyOCH_3$·HCl) were prepared according to literature procedures. Toluene was refluxed with sodium, and CH_2Cl_2 dried with CaH. The dry solvents were distilled and storage in ample under the protection of N_2 (99.999%).

Typical procedure for preparation and characterization of complexes 3a-3g

$[Ru_2(CO)_4(\mu^2\text{-}\eta^2\text{-}O_2CCH_3)_2\ (\eta^1\text{-}NH_2CH_2C(=O)OCH_3)_2]$ (3a). The thermolysis of $Ru_3(CO)_{12}$ and carboxylic acid in toluene at 110-130°C afforded the pale yellow solution of $[Ru_2(O_2CCH_3)_2(CO)_4]_n$ **(a)** along with byproduct CO and H_2. The reaction mixture was cooled down 0 °C. Two equivalents of HCl·GlyOMe (0.93 mmol) were neutralized by triethylamine in CH_2Cl_2, and were added to the above reaction mixture via cannula filtration. The resultant mixture was stirred at 110 °C for 2 h. The bright pale yellow solution was then briefly cooled, and the solvent was removed under vacuum. The crude powder product was recrystallized as yellow prismatic crystals, 247mg (yield 87%). IR (CH_3OH, cm^{-1}): ν_{co}=2026vs, 1972m, 1941vs, $\nu(CO_2)$=1749m, ν_{acid}=1580m; ^1H NMR(400 MHz, $CDCl_3$): δ(ppm) 1.96(s, 6H, CH_3CO_2), 2.87(t, 4H, NH_2), 3.72(t, 4H, CH_2), 3.80(s, 6H, CO_2CH_3), ^{13}C NMR(100MHz, $CDCl_3$): δ(ppm) 204(CO), 184(CO_2CH_3), 172(CH_3CO_2), 52(CO_2CH_3), 46(CH_2), 23(CH_3CO_2).

$[Ru_2(CO)_4(\mu^2\text{-}\eta^2\text{-}O_2CCH_3C_6H_4)_2(\eta^1NH_2CH_2C(=O)OCH_3)_2]$ (3b). Yellow prismatic crystals. Yield: 286mg (81%). IR (CH3OH, cm^{-1}): ν_{co}=2025vs, 1972m, 1941vs, V(CO_2)=1749m, Vacid=1594m; ^1H NMR(400 MHz, $CDCl_3$): δ(ppm) 7.76(d, 4H, Ph), 7.12(d, 4H, Ph), 2.34(s, 6H, CH_3), 3.14(t, 4H, NH_2), 3.90(t, 4H, CH_2), 3.86(s, 6H, CO_2CH_3), ^{13}C NMR(100MHz, $CDCl_3$): δ(ppm) 204(CO), 179(CO_2CH_3), 172($PhCO_2$), 142(Ph), 130(Ph), 129(Ph), 128(Ph), 52(CO_2CH_3), 46(CH_2), 21(CH_3).

$[Ru_2(CO)_4(\mu^2\text{-}\eta^2\text{-}O_2C\text{-}p\text{-}ClC_6H_4)_2(\eta^1\text{-}NH_2CH_2C(=O)OCH_3)_2]$ (3c). Deep yellow powder. Yield: 291mg (78%). IR (CH_3OH, cm^{-1}): ν_{co}=2027vs, 1974m, 1944vs, $\nu(CO_2)$=1749m, ν_{acid}=1597m ; ^1H NMR(400 MHz, $CDCl_3$): δ(ppm) 7.81(d, 4H, Ph), 7.28(d, 4H, Ph), 3.14(t, 4H, NH_2), 3.88(t, 4H, CH_2), 3.85(s, 6H, CO_2CH_3), ^{13}C NMR(100MHz, $CDCl_3$): δ(ppm) 203(CO), 178(CO_2CH_3), 172($PhCO_2$), 138(Ph), 131(Ph), 130(Ph), 128(Ph), 53(CO_2CH_3), 46(CH_2).

$[Ru_2(CO)_4(\mu^2\text{-}\eta^2\text{-}O_2C\text{-}p\text{-}CH_3OC_6H_4)_2(\eta^1NH_2CH_2C(=O)OCH_3)_2]$ (3d). Yellow prismatic crystals. Yield: 310mg (84%). IR (CH_3OH, cm^{-1}): ν_{co}=2024vs, 1971m, 1941vs, $\nu(CO_2)$=1749m, Vacid=1595m; ^1H NMR(400 MHz, $CDCl_3$): δ(ppm) 7.81(d, 4H, Ph), 6.82(d, 4H, Ph), 3.81(s, 6H, CH_3O), 3.13(t, 4H, NH_2), 3.91(t, 4H, CH_2), 3.86(s, 6H, CO_2CH_3), ^{13}C NMR(100MHz, $CDCl_3$): δ(ppm) 204(CO), 178(CO_2CH_3), 172($PhCO_2$), 162(Ph), 131(Ph), 126(Ph), 113(Ph), 55(OCH_3), 53(CO_2CH_3), 46(CH_2).

$[Ru_2(CO)_4(\mu^2\text{-}\eta^2\text{-}O_2CC_6H_5)_2(\eta^1\text{-}NH_2CH_2C(=O)OCH_3)_2]$ (3e). Yellow prismatic crystals. Yield: 293mg (86%). IR (CH_3OH, cm^{-1}): ν_{co}=2026vs, 1973m, 1943vs, $\nu(CO_2)$=1749m, ν_{acid}=1560m; ^1H NMR(400 MHz, $CDCl_3$): δ(ppm) 7.87(d, 4H, Ph), 7.43(d, 4H, Ph), 7.32(t, 4H, Ph), 3.16(t, 4H, NH_2), 3.90(t, 4H, CH_2), 3.85(s, 6H, CO_2CH_3), ^{13}C NMR(100MHz, $CDCl_3$): δ(ppm) 204(CO), 178(CO_2CH_3), 172(CH_3CO_2), 133(Ph), 132(Ph), 129(Ph), 128(Ph), 53(CO_2CH_3), 46(CH_2).

$[Ru_2(CO)_4(\mu^2\text{-}\eta^2\text{-}O_2C\text{-}o\text{-}CH_3C_6H_4)_2(\eta^1\text{-}NH_2CH_2C(=O)OCH_3)_2]$ (3f). Deep yellow powder. Yield: 297mg (84%). IR (CH_3OH, cm^{-1}): ν_{co}=2027vs, 1973m, 1943vs, $\nu(CO_2)$=1749m, ν_{acid}=1584m ; ^1H NMR(400 MHz, $CDCl_3$): δ(ppm) 7.61(d, 2H, Ph), 7.30(t, 2H, Ph), 7.15(dd, 4H, Ph), 2.41(s, 6H, CH_3), 3.04(t, 4H, NH_2), 3.82(t, 4H, CH_2), 3.78(s, 6H, CO_2CH_3), ^{13}C NMR(100MHz, $CDCl_3$): δ(ppm) 204(CO), 181(CO_2CH_3), 172($PhCO_2$), 137(Ph), 134(Ph), 131(Ph), 130(Ph), 129(Ph), 125(Ph), 52(CO_2CH_3), 46(CH_2), 22(CH_3).

$[Ru_2(CO)_4(\mu^2\text{-}\eta^2\text{-}O_2C\text{-}m\text{-}CH_3C_6H_4)_2(\eta^1\text{-}NH_2CH_2C(=O)OCH_3)_2]$ (3g). Yellow prismatic crystals. Yield: 261mg (74%). IR (CH_3OH, cm^{-1}): ν_{co}=2026vs, 1972m, 1942vs, $\nu(CO_2)$=1749m, Vacid=1596m; ^1H NMR(400 MHz, $CDCl_3$): δ(ppm) 7.60(d, 4H, Ph), 7.19(d, 2H, Ph), 7.14(dd, 2H, Ph), 2.27(s, 6H, CH_3), 3.04(t, 4H, NH_2), 3.85(t, 4H, CH_2), 3.78(s, 6H, CO_2CH_3), ^{13}C NMR(100MHz, $CDCl_3$): δ(ppm) 204(CO), 179(CO_2CH_3), 172($PhCO_2$), 138(Ph), 133(Ph), 132(Ph), 130(Ph), 129(Ph), 127(Ph), 52(CO_2CH_3), 46(CH_2), 21(CH_3).

Acknowledgements

We acknowledge the 111 Project (B14041), Innovative Research Team in University of China (IRT1070), the grant from National Natural Science Foundation of China (21371112), the grant from Fundamental Doctoral Fund of Ministry of Education of China (20120202120005), the Fundamental Funds Research for the Central Universities (GK201501005), Shaanxi Innovative Team of Key Science and Technology (2013KCT-17) and Natural Science Basic Research Plan in Shaanxi Province of China (2012JM2006) for financial support.

Notes and references

1 Recent progress on CORM: (a) S. García-Gallego, G. J. L. Bernardes, *Angew. Chem. Int. Ed.*, 2014, **53**, 9712-9721; (b) U. Schatzschneider, *Br. J. Pharmacol*, 2014, **172**, 1638-1650.

2 Concepts of PhotoCORM: (a) I. Chakraborty, S. J. Carrington, P. K. Mascharak, *Acc. Chem. Res.*, 2014, **47**, 2603-2611; (b) R. D. Rimmer, A. E. Pierri and P. C. Ford, Coord. *Chem. Rev.*, 2012, **256**, 1509-1519; (c) U. Schatzschneider, *Inorg. Chim. Acta*, 2011, **374**, 19-23.

3 (a) J. D. Seixas, A. Mukhopadhyay, T. Santos-silva, L. E. Otterbein, D. J. Gallo, S. S. Rodrigues, B. H. Guerreiro, A. M. L. Goncalves, N. Penacho, A. R. Marques, A. C. Coelho, P. M. Reis, M. J. Romão and C. C. Romão, *Dalton Trans.*, 2013, **42**, 5985-5998; (b) L. Hewison, T. R. Johnson, B. E. Mann, A. J. H. M. Meijer, P. Sawle and R. Motterlini, *Dalton Trans.*, 2011, **40**, 8328-8334; (c) R. Kretschmer, G. Gessner, H. Görls, S. H. Heinemann and M. Westerhausen, *J. Inorg. Biochem*, 2011, **105**, 6-9.

4 (a) J. D. Seixas, M. F. A. Santos, A. Mukhopadhyay, A. C. Coelho, P. M. Reis, L. F. Veiros, A. R. Marques, N. Penacho, A. M. L. Gonçalves, M. J. Romão, G. J. L. Bernardes, T. Santos-Silva and C. C. Romão, *Dalton Trans.*, 2015, **44**, 5058-5075; (b) S. Pai, M. Hafftlang, G. Atongo, C. Nagel, J. Niesel, S. Botov, H. G. Schmalz, B. Yard and U. Schatzschneider, *Dalton Trans.*, 2014, **43**, 8664-8678. (c) J. D. Compain, M. Bourrez, M. Haukka, A. Deronzier and S. Chardon-Noblat, *Chem. Comm.*, 2014, **50**, 2539-2542; (d) S. J. Carrington, I. Chakraborty and P. K. Mascharak, *Chem. Comm.*, 2013, **49**, 11254-11256; (e) M. A. Gonzalez, S. J. Carrington, N. L. Fry, J. L. Martinez and P. K. Mascharak, *Inorg. Chem.*, 2012, **51**, 11930-11940; (f) M. A. Gonzalez, M. A. Yim, S. Cheng, A. Moyes, A. J. Hobbs and P. K. Mascharak, *Inorg. Chem.*, 2012, **51**, 601-608; (g) C. S. Jackson, S. Schmitt, Q. P. Dou and J. J. Kodanko, *Inorg. Chem.*, 2011, **50**, 5336-5338.

5 (a) A. E. Pierri, A. Pallaoro, G. Wu and P. C. Ford, *J. Am. Chem. Soc.*, 2012, **134**, 18197-18200; (b) W. Q. Zhang, A. J. Atkin, I. J. S. Fairlamb, A. C. Whitwood and J. M. Lynam, *Organometallics*, 2011, **30**, 4643-4654; (c) S. H. Crook, B. E. Mann, A. J. H. M. Meijer, H. Adams, P. Sawle, D. Scapens, and R. Motterlini, *Dalton Trans.*, 2011, **40**, 4230-4235; (d) W. Q. Zhang, A. C. Whitwood, I. J. S. Fairlamb and J. M. Lynam, *Inorg. Chem.*, 2010, **49**, 8941-8952;(e) R. D. Rimmer, H. Richter and P. C. Ford, *Inorg. Chem.*, 2010, **49**, 1180-1185.

6 (a) F. Zobi, L. Quaroni, G. Santoro, T. Zlateva, O. Blacque, B. Sarafimov, M. C. Schaub and A. Y. Bogdanova, *J. Med. Chem.*, 2013, **56**, 6719-6731; (b) F. Zobi, O. Blacque, R. A. Jacobs, M. C. Schaub, and A. Y. Bogdanova, *Dalton Trans.*, 2012, **41**, 370-378; (c) J. B. Matson, M. J. Webber, V. K. Tamboli, B. Weber and S. I. Stupp, *Soft Matter*, 2012, **8**, 2689-2692; (d) U. Hasegawa, A. J. van der Vlies, E. Simeoni, C. Wandrey and J. A. Hubbell, *J. Am. Chem. Soc*, 2010, **132**, 18273-18280; (e) H. Pfeiffer, A. Rojas, J. Niesel and U. Schatzschneider, *Dalton Trans.*, 2009, 4292-4298.

7 (a) C. C. Romão, W. A. Blättler, J. D. Seixas and G. J. L. Bernardes, *Chem. Soc. Rev.*, 2012, **41**, 3571-3583; (b) R. Motterlini and L. E. Otterbein, *Nat. Rev. Drug Discov.*, 2010, **9**, 728-743; (c) R. Alberto and R. Motterlini, *Dalton Trans.*, 2007, **17**, 1651-1660.

8 T. R. Johnson, B. E. Mann, J. E. Clark, R. Foresti, C. J. Green, and R. Motterlini, *Angew. Chem. Int. Ed.*, 2003, **42**, 3722-3729.

9 (a) H. Song, C. Bergstrasser, N. Rafat, S. Höger, M. Schmidt, N. Endres, M. Goebeler, J. L. Hillebrands, R. Brigelius-Flohé, A. Banning, G. Beck, R. Loesel and B. A. Yard, *Br. J. Pharmacol*, 2009, **157**, 769-780; (b) P. Sawle, R. Foresti, B. E. Mann, T. R. Johnson, C. J. Green and R. Motterlini, *Br. J. Pharmacol*, 2005, **145**, 800-810.

10 P. Wang, H. Liu, Q. Zhao, Y. Chen, B. Liu, B. Zhang and Q. Zheng, *Europ. J. Med. Chem.*, 2014, **74**, 199-215.

11 A. R. Marques, L. Kromer, D. J. Gallo, N. Penacho, S. S. Rodrigues, J. D. Seixas, G. J. L. Bernardes, P. M. Reis, S. L. Otterbein, R. A. Ruggieri, A. S. G. Gonçalves, A. M. L. Gonçalves, M. N. D. Matos, I. Bento, L. E. Otterbein, W. A. Blättler and C. C. Romão, *Organometallics*, 2012, **31**, 5810-5822.

12 J. Niesel, A. Pinto, H. W. P. N'Dongo, K. Merz, I. Ott, R. Gust and U. Schatzschneider, *Chem. Comm.*, 2008, 1798-1800.

13 R. Foresti, J. Hammad, J. E. Clark, T. R. Johnson, B. E. Mann, A. Friebe, C. J. Green and R. Motterlini, *Br. J. Pharmacol*, 2004, **142**, 453-460.

14 (a) T. Santos-Silva, A. Mukhopadhyay, J. D. Seixas, G. J. L. Bernardes, C. C. Romão and M. J. Romão, *J. Am. Chem. Soc.*, 2011, **133**, 1192-1195; (b) T. R. Johnson, B. E. Mann, I. P. Teasdale, H. Adams, R. Foresti, C. J. Green and R. Motterlini, *Dalton Trans.*, 2007, 1500-1508.

15 J. Johnpeter, L. Plasseraud, F. Schmitt, L. J. Jeanneret and B. Therrien, *J. Coord. Chem.*, 2013, **66**, 1753-1762.

16 B. Therrien and G. Süss-Fink, *Coord. Chem. Rev.*, 2009, **253**, 2639-2664.

17 (a) F. Schmitt, M. Auzias, P. Štěpnička, Y. Sei, K. Yamaguchi, G. Süss-Fink, B. Therrien and L. Juillerat-Jeanneret, *J. Biol. Inorg. Chem.*, 2009, **14**, 693-701; (b) M. Gras, N. P. E. Barry, B. Therrien and G. Süss-Fink, *Inorg. Chim. Acta.*, 2011, **371**, 59-62.

18 C. S. Jackson, S. Schmitt, Q. P. Dou and J. J. Kodanko, *Inorg. Chem.*, 2011, **50**, 5336-5338.

Photo-activated CO-Releasing Molecules (PhotoCORMs) of Robust Sawhorse Scaffolds [μ^2-OOCR^1, η^1-$NH_2CHR^2(C=O]OCH_3$, $Ru(I)_2CO_4$]

Shuhong Yang, Mengjiao Chen, Lingling Zhou, Guofang Zhang, Ziwei Gao and Weiqiang Zhang*

Simple is the best: by nature abundant small organics and low toxicity transition metal, stable sawhorse-type $Ru_2(CO)_4$complexes were synthesized, characterized and validated as a lead structure for photo-activated CO-releasing molecules (Photo CORM).